Why do tornados and hailstorms rest on weekends?

Daniel Rosenfeld[1] and Thomas L. Bell[2]

Received 5 May 2011; revised 4 August 2011; accepted 4 August 2011; published 27 October 2011.

[1] This study shows for the first time statistical evidence that when anthropogenic aerosols over the eastern United States during summertime are at their weekly mid-week peak, tornado and hailstorm activity there is also near its weekly maximum. The weekly cycle in summertime storm activity for 1995–2009 was found to be statistically significant and unlikely to be due to natural variability. It correlates well with previously observed weekly cycles of other measures of storm activity. The pattern of variability supports the hypothesis that air pollution aerosols invigorate deep convective clouds in a moist, unstable atmosphere, to the extent of inducing production of large hailstones and tornados. This is caused by the effect of aerosols on cloud drop nucleation, making cloud drops smaller and hydrometeors larger. According to simulations, the larger ice hydrometeors contribute to more hail. The reduced evaporation from the larger hydrometeors produces weaker cold pools. Simulations have shown that too cold and fast-expanding pools inhibit the formation of tornados. The statistical observations suggest that this might be the mechanism by which the weekly modulation in pollution aerosols is causing the weekly cycle in severe convective storms during summer over the eastern United States. Although we focus here on the role of aerosols, they are not a primary atmospheric driver of tornados and hailstorms but rather modulate them in certain conditions.

Citation: Rosenfeld, D., and T. L. Bell (2011), Why do tornados and hailstorms rest on weekends?, *J. Geophys. Res.*, *116*, D20211, doi:10.1029/2011JD016214.

1. Introduction

[2] This study puts to a statistical test the hypothesis that air pollution increases the chance of severe convective storms. The motivation for posing this question is based on physical considerations that are described in section 1.2. These considerations have already been partially supported by the observations of a weekly cycle in rainfall, storm heights, and large-scale vertical winds, made by *Bell et al.* [2008]. We believe this hypothesis does two things: (1) it provides a framework for understanding the observations originally reported by *Bell et al.* [2008] and (2) it has been a very successful tool for predicting weekly cycles in other meteorological quantities, some of which have been reported elsewhere (e.g., lightning activity [*Bell et al.*, 2009a]), and fractional cloud cover and cloud top temperatures (mentioned by *Bell et al.* [2009b]), and some of which (weekly cycles in hailstorm and tornado activity) are reported here.

[3] We believe that a strong observational case is made in this paper for the existence of a weekly cycle in hailstorm and tornado activity over the eastern United States during the summer. We would not have looked for such evidence had we not had the physical theory we present below to guide us. Nevertheless, we should emphasize that the observations we report here only show a correlation in hailstorm and tornado activity with the well-established weekly cycle in pollution over the same area, and correlations do not prove causality. These observations provide the impetus for more detailed observational studies and advances in modeling of the effects of aerosols on storm development that will be capable of establishing the causal connection, a connection we can only present as a hypothesis here.

1.1. The Weekly Cycle in Rain Intensity and Lightning Activity

[4] The weekly cycle of working weekdays and resting weekends is associated with weekly varying levels of particulate air pollution [e.g., *Bell et al.*, 2008]. This cycle has been shown to be associated with weekly cycles of midweek rainfall amounts, storm heights [*Bell et al.*, 2008, 2009b], and lightning activity [*Bell et al.*, 2009a] in the warm and moist climate of summer months in the southeast United States. It was hypothesized that this is caused by mid-week enhanced particulate air pollution invigorating convective storms, as will be described in section 1.2. Theoretical considerations and cloud simulations, described in section 1.3, support this hypothesis.

1.2. The Physical Basis for Aerosols Invigorating Convective Clouds

[5] Particulate air pollution can invigorate convective storms whose cloud bases are warm enough that the cloudy

[1]Institute of Earth Sciences, The Hebrew University of Jerusalem, Jerusalem, Israel.
[2]Climate and Radiation Branch, NASA Goddard Space Flight Center, Greenbelt, Maryland, USA.

Copyright 2011 by the American Geophysical Union.
0148-0227/11/2011JD016214

air has to rise several km before reaching the freezing level. In clouds forming in pollution-free air, rain can develop and precipitate from the lower parts of the cloud without freezing. This early rain can be inhibited by the pollution aerosol particles that act as cloud drop condensation nuclei (CCN) and nucleate greater concentrations of smaller cloud drops that are slower to coalesce into raindrops [*Gunn and Phillips*, 1957]. In clouds with warm cloud base temperatures the freezing level is several km above cloud base, so that rain can develop and fall from the rising air in the cloud. Because the effect of aerosols is to suppress coalescence, rain is delayed and a larger fraction of the cloud water ascends above the 0°C isotherm level, where it is accreted on ice precipitation particles that fall and melt at lower levels [*Molinié and Pontikis*, 1995; *Andreae et al.*, 2004]. The additional release of latent heat of freezing aloft and reabsorbed heat at lower levels by the melting ice implies greater upward heat transport for the same amount of surface precipitation in the more polluted atmosphere. In addition, greater evaporative cooling of the cloud water in the downdrafts increases further the vertical heat exchange [*Lee et al.*, 2010]. This means that more instability is consumed for the same amount of rainfall. The inevitable outcome is invigoration of the convective clouds [*Rosenfeld et al.*, 2008]. Cloud simulations have supported this hypothesis by showing that updrafts increase in warm-base clouds (~20°C) with added aerosols that suppress the warm-rain processes [*Khain and Pokrovsky*, 2004, 2005, 2008; *Khain and Lynn*, 2009; *Wang*, 2005; *Tao et al.*, 2007; *Li et al.*, 2008; *Lee et al.*, 2008a; *van den Heever et al.*, 2006; *van den Heever and Cotton*, 2007; *Ntelekos et al.*, 2009]. According to these simulations, invigoration was not necessarily associated with added rainfall amounts. Enhanced rainfall was simulated only in warm, moist, unstable, and low-shear environments [*Khain et al.*, 2008; *Lee et al.*, 2008b; *Fan et al.*, 2007, 2009]. The stronger updrafts and downdrafts resulted in more coherent organization of the simulated convection that feeds back into the intensity of the storms [*Ntelekos et al.*, 2009; *Lee et al.*, 2010]. The invigoration was supported also by observations of more polluted convective clouds growing taller [*Koren et al.*, 2005, 2008, 2010] and invigorating the circulation systems [*Zhang et al.*, 2007; *Bell et al.*, 2008].

1.3. The Physical Basis for Aerosols Enhancing Lightning, Hail, and Tornados

[6] The invigorated updrafts with added supercooled water and ice hydrometeors provide the conditions for enhanced cloud electrification [*Molinié and Pontikis*, 1995; *Williams et al.*, 2002; *Andreae et al.*, 2004]. However, the observational evidence was questioned due to the difficulty in separating the roles of thermodynamics and aerosols [*Lyons et al.*, 1998; *Williams and Stanfill*, 2002; *Williams et al.*, 2002; *Williams*, 2005]. Critical supporting observational evidence for the validity of the invigoration hypothesis was obtained very recently, where volcanic aerosols, whose variability was completely independent of meteorology, were observed to invigorate deep convective clouds over the northwest subtropical Pacific Ocean and more than double the lightning activity [*Yuan et al.*, 2011; *Langenberg*, 2011].

[7] The greater amount of supercooled cloud water in polluted situations means greater growth rate of ice hydrometeors. The stronger updrafts mean that larger hail stones can be suspended in the cloud before falling to the ground. Therefore, it is reasonable to expect that clouds in more polluted air would produce larger hail stones. This is supported by some observations [*Andreae et al.*, 2004; *Wang et al.*, 2009] and simulations [*Storer et al.*, 2010; *Khain et al.*, 2011].

[8] The dynamics of convective storms respond to the initial changes in precipitation by changes in the downdrafts and their evaporative cooling, which feed the cold pools and their gust fronts. Early simulations [*Gilmore et al.*, 2004; *van den Heever and Cotton*, 2004] showed that storm dynamics are very sensitive to changes in hydrometeor size, such that smaller hydrometeors create larger cold pools and stronger gust fronts that feed back to the storm dynamics. Colder downdrafts would produce a faster moving gust front that would tend to cause faster propagation of the squall line. A supercell can be regarded as a quasi steady state convective storm, where the gust front is not outrunning and undercutting the updraft in the feeder clouds. Less evaporative cooling into the downdraft would reduce the cooling and extent of the cold pool. A slower-moving gust front with respect to its originating cell would drive the convective system closer to a state of a supercell, which is the typical cloud type that produces large hail and tornados.

[9] Supercell storms inherently form in a high–wind shear environment. The wind shear causes the main rain shaft with the associated downdraft to be displaced from the low-level updraft. This is the mechanism that allows the longevity of the supercell storms, and hence increases their vigor and potential for generating tornados and large hail. The simulations of *Fan et al.* [2009] showed that aerosol-induced invigoration of the updraft aloft requires a weak wind shear environment. With little aerosol-induced invigoration expected during the strong–wind shear conditions that are favorable for large hail and tornadic storms, the mechanism in question by which aerosols increase the chance of tornados, cannot be fully explained by the convective invigoration hypothesis [*Rosenfeld et al.*, 2008]. Here we propose that the aerosol-induced changes in the precipitation particle size distribution reduce the evaporative cooling in the precipitation shaft. The way by which it might enhance tornadogenesis is described next.

[10] *Ludlam* [1963] proposed that air parcels within the downdraft tend to be less negatively buoyant (warmer) in tornadic versus nontornadic supercells. Tornadic vortices increase in intensity and longevity as downdraft parcel buoyancy increases, because colder parcels are more resistant to lifting. This was supported by observational and numerical modeling studies [*Markowski et al.*, 2002, 2003]. Simulations of the sensitivity of tornadogenesis to the hydrometeor size distribution, done at the high resolution of 100 m [*Snook and Xue*, 2008], showed that by merely increasing the hydrometeor size an EF-2 intensity tornado was produced by the model. When the cold pool is strengthened by decreasing the hydrometeor sizes, the updraft is tilted rearward by the strong, surging gust front, causing a disconnection between low-level circulation centers near the gust front and the mid-level mesocyclone.

[11] Clouds with smaller drops were observed to produce larger raindrops for the same rain intensity [*Rosenfeld and Ulbrich*, 2003]. This was confirmed by simulations of warm rain [*Altaratz et al.*, 2008] and mixed phase clouds [*Khain*

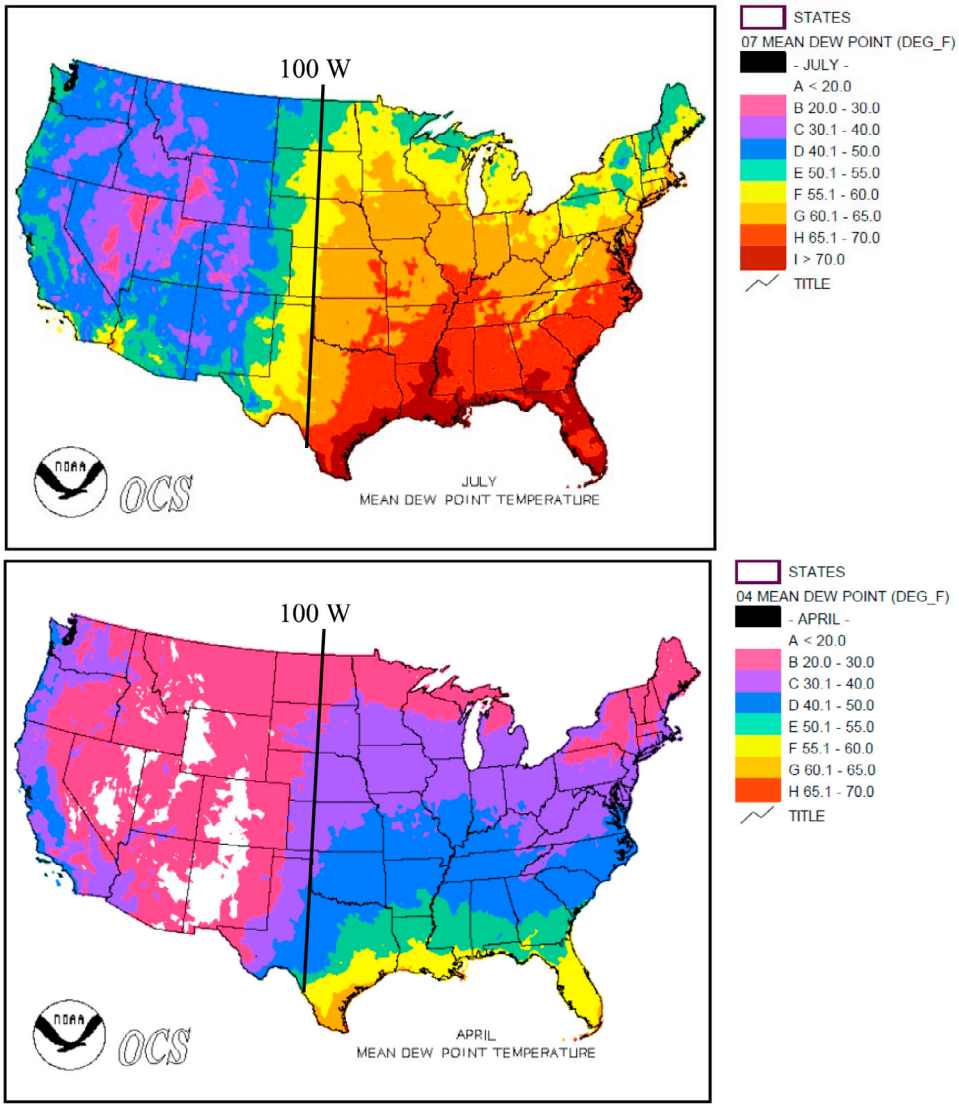

Figure 1. Mean dew point temperature for (top) July and (bottom) April. From the National Oceanic and Atmospheric Administration Climatic Data Center.

et al., 2011]. Incorporating this effect in simulations of an idealized supercell thunderstorm [*Lerach et al.*, 2008] showed that the added aerosols suppressed the precipitation and produced larger and fewer hailstones and raindrops. This produced an EF-1 tornado. The unpolluted simulation produced more precipitation evaporative cooling, and thus a stronger surface cold pool that surged and destroyed the rear flank downdraft structure. This resulted in a single gust front that propagated more rapidly away from the storm system, separating the low-level vorticity source from the parent storm and thus hindering the tornadogenesis.

[12] *Rosenfeld and Ulbrich* [2003] attributed the aerosol effect on precipitation particle size distribution to the larger number of raindrop embryos that form in warm rain processes as compared to precipitation initiation by ice precipitation embryos in mixed phase clouds. For the same aerosol concentrations, warmer cloud base means larger distance to the freezing level, where cloud drops can grow bigger and coalesce faster into raindrops. Therefore, this aerosol effect on the precipitation particle size distribution and in turn on tornadogenesis is expected to be more pronounced for clouds with warmer bases. According to Figure 1, sufficiently warm cloud base for the aerosol effects (>~15°C) occur during the months June–August over the eastern part of the United States, to the east of longitude 100°W. During the summer months this line lies along the dew point isotherm of 15°C within a sharp gradient of increasing dew points eastward. The analysis of the aerosol effects in this study is focused at these times and places. Interestingly, the strongest hailstorms occur just to the west of 100°W. *Williams et al.* [2005] ascribed this to the fact that cloud base height is sufficiently high and cold while the instability is still very high, such that warm rain is prevented from forming in the short distance between cloud base and the freezing level regardless of the aerosol amounts, allowing large accumulations of supercooled water that feed the growth of large hail. The cloud base is still not too cold to deplete the amount of potential condensates and supercooled water that are required for the

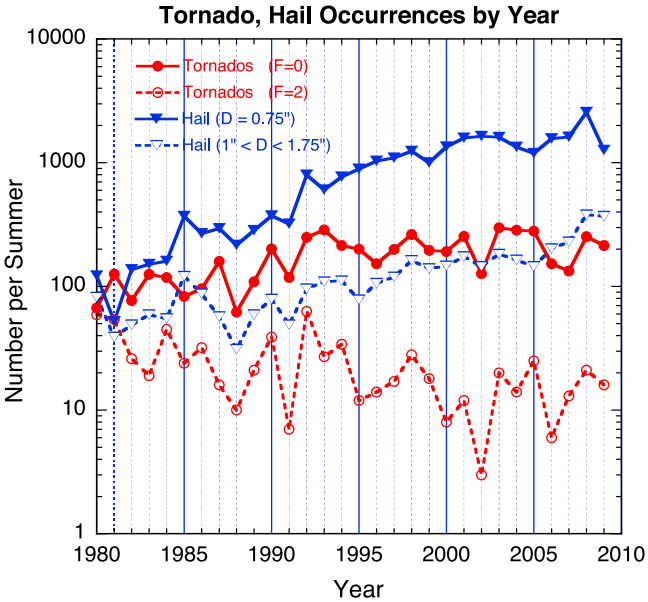

Figure 2. Number of tornado and hailstorm events each summer (June–August) for 1980–2009. Graphs are shown for tornados classified as F0 and as F2 in strength and for hailstorms with reported hail diameters of 0.75 inches and between 1 and 1.75 inches (exclusive). (Because hail diameters are generally given in 0.25 inch increments, this bin includes mostly hail diameters of 1.25 and 1.5 inches.)

growth of large hail. The cloud base west of 100°W is thus too cool for aerosols to be a major factor in modulating the hailstorms.

[13] In this brief review we have shown that there is a physical basis for the hypothesis that added aerosols can contribute to the occurrence of large hail and tornados. In the next sections the hypothesis that the weekly cycle in pollution aerosols is associated with a similar cycle in the hail and tornados will be tested using observational data for hail and tornado activity.

2. The Data

[14] On the basis of the physical considerations above, we expect that the occurrences of severe convective storms would be enhanced in a more polluted atmosphere during the summer months in the eastern United States, where the convective storms form in a warm and moist atmosphere and are least forced by synoptic weather systems such as cold fronts. In order to test whether there is a weekly cycle, daily counts of tornados or hail, categorized by intensity, were analyzed.

[15] Data for tornado and hail observations in the United States were obtained from the Web site of the Storm Prediction Center (SPC) of the National Oceanic and Atmospheric Administration (see http://www.spc.noaa.gov/wcm/index.html#data). The observational data maintained by the SPC are based on reports collected by local National Weather Service Forecast Offices from a wide variety of sources (trained spotters, emergency personnel, the media, the general public, etc.). The assignment of tornado strength on the enhanced Fujita scale (http://www.spc.noaa.gov/efscale/) for a tornado probably reflects both estimates of the intrinsic strength of the tornado and valuations of the level of property damage found along the path of the tornado [see, e.g., *Doswell and Burgess*, 1988]. A characteristic largest hailstone size is assigned to hailstorm events, according to the National Oceanic and Atmospheric Administration (NOAA) National Weather Service storm data preparation rules (see http://www.weather.gov/directives/sym/pd01016005curr.pdf). Hail diameters are given in inches. One inch equals 2.54 cm. The NOAA Warning Coordination Meteorologist attempts to identify and remove duplicate observations and to link storms that span several jurisdictions. The data we used were current as of 16 March 2010.

[16] *Schaefer and Edwards* [1999] suggest a number of possible biases in these data: tornados generally go unreported where no one lives; both population and population awareness has increased over the years; and the adoption of warning systems has made people more alert to tornados. More tornados are observed near populated areas than away from them. Storms that are particularly severe are probably missed less often, however. The total numbers of tornados and of hailstorms have generally trended upward with the years (Figure 2). The conventions for attributing a given Fujita scale to a storm have also evolved [e.g., *Schaefer and Edwards*, 1999]. Rapid increases in the numbers reported may be due to the introduction of new technology: implementation of the WSR-88D radars with Doppler capability in about 1991, for example, may have led to increased reporting of tornados after that date. An analysis by *Ray et al.* [2003] suggests that tornados are reported more often near population centers and that tornado occurrences prior to 1992 may have been underestimated by about 40%.

[17] The observational biases that may be present in the data can easily be imagined to change with the day of the week. Weekly changes in media coverage are possible, for instance. Despite these possibilities, we report later in the paper that we see no signs of a weekly cycle in the less populated western half of the United States and no signs of a cycle during the spring season in the eastern half. It is not easy to think of a plausible sociological bias that is present in the eastern half of the country but absent in the western half, or one that is absent in the spring and then appears in the summer. We also find that the weekly cycle in tornado and hail activity seen in the eastern half of the United States agrees well with the weekly cycle seen in other indicators of severe storm activity such as lightning and extent of vertical development of the storm clouds (indicators that are not subject to the same concerns about weekly biases in the observational system). These same indicators show no significant weekly cycle in the western half of the United States [*Bell et al.*, 2008, 2009a, 2009b]. This suggests that whatever physical mechanisms are modulating severe storm activity in the east during the summer are also affecting tornado and hail activity. The evidence we report here strongly suggests, we believe, that the weekly cycles in tornado and hail activity are real. Attempts to explain them as simply the result of weekly shifts in coverage by the observational network require constructing a rather tortuous and contrived picture of societal behavior.

[18] In preparing the data for analysis, we edited a small fraction of the data entries based on the recommendations accompanying the data provided by the SPC and on the

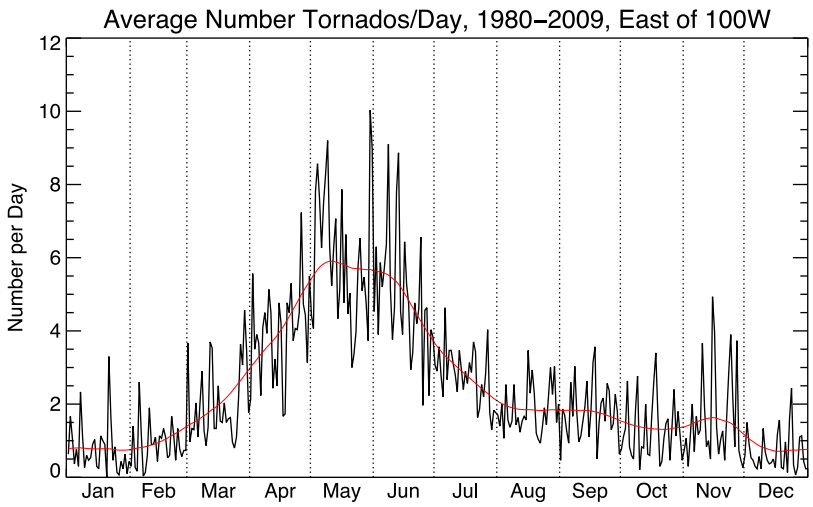

Figure 3. Average number of tornados per day (jagged black curve), all strengths, for years 1980–2009. The smooth red curve shows fit to data using a Lee filter, as described in the text, and was used by us as the expected tornado count for days of the year. It is denoted by $f(j)$ in the text.

need to resolve various ambiguities. Entries with missing state identifications were ignored. Entries with either zero latitude or longitude locations were ignored. Entries with negative Fujita scales were ignored (25 cases encountered). Apparently misidentified time zones were corrected. Multiple entries associated with a single tornado event were consolidated into one entry (not an issue in the hail data set). Tornados that crossed state boundaries were treated as two separate events, however. Fifteen entries of hail sizes of 0.25 and 0.5 inches in 2007 were pooled with the entries for 0.75 inches. In total, fewer than 2% of the tornado data set entries required editing. A far smaller percentage of hail data entries required editing. The number of tornado events for 1980–2009 in our edited data set was approximately 33,000, while the number of hail events was approximately 235,000.

3. The Data Analysis

[19] In the following subsections we provide details about the assumptions and methods used in the statistical analysis of the tornado and hailstorm data.

3.1. Statistical Model of Data Under the Null Hypothesis

[20] Testing the data for the presence of a weekly cycle requires a description of the statistics of the data under the null hypothesis, which is that the frequency of tornados or hailstorms does not vary cyclically with the day of the week. In modeling the statistics of hailstorms and tornado occurrences under the null hypothesis, we try to accommodate the known variations in statistics with the season and year. Our goal is not to determine the "true" seasonal cycle or decadal trend but simply to produce something likely to be closer to the truth than ignoring the seasonal cycle or year-by-year trend altogether.

[21] We used the average seasonal cycle over the years 1980–2009 to represent the modulation of the expected count with the seasons (i.e., with the day of the year). Though we used 15 years of data (1980–1994) prior to the period we are concentrating on (1995–2009), they were used only to help establish the background seasonal cycles and decadal-scale trends, and for the bootstrap statistical analysis described later. The seasonal cycle estimated from 30 years of data is smoother than the cycle estimated using 15 years (1995–2009), as would be expected, but is not substantially different. We believe that using data prior to 1995–2009 to increase the stability of our estimate of the seasonal cycle increases the overall robustness of our statistics, but that if we had confined our averaging to the years 1995–2009 our conclusions would not be changed in any substantial way.

[22] We show in Figure 3 the average number of tornados reported east of longitude 100°W for each day of the year. The averages for each day of the year in Figure 3, though based on 30 years of data, exhibit quite a lot of variability from day to day, almost certainly due to the sample size (30 samples, one for each year) in the daily averages. Note that averages for each day of the year include data from all days of the week (Sunday through Saturday). Rather than trying to build a smoother, parameterized model for the seasonal cycle, we applied a kind of running average to the 365 daily averages (leap years treated as having 365 days). The filter devised by *Lee* [1986] produced a satisfactory curve when we applied the filter twice with a window size of 11 days (on either side of the central value), as shown in Figure 3. The Lee filter produces a smooth fit to the data but tries also to capture sudden jumps in the local mean. The climatological average compares well to the average obtained by *Brooks et al.* [2003], though *Brooks et al.* [2003] report averages for a different region and time period.

[23] The annual counts for each year from 1980 to 2009 vary quite a bit from year to year (e.g., see Figure 2), possibly attributable to large-scale influences such as El Niño–Southern Oscillation or to the unpredictable fluctuations in weather, but there appears to be a decadal trend in the counts as well. Some of these trends might be explained by societal changes, such as increasing awareness of the danger of tornados, and in the methods of collecting the data, as discussed by *Schaefer and Edwards* [1999].

[24] We found that the seasonal cycles of the different tornado strengths are fairly similar (although the small numbers of high-EF tornados make comparisons of averages difficult), when the seasonal cycle of counts for a particular EF values is normalized by the total number of storms at that EF value. The seasonal cycles for different hail sizes are very similar. We should note, however, that the similarity in the seasonal cycles is used very little in the analyses presented here.

[25] In order to test whether the tornado/hailstorm statistics differ significantly from what would be expected under the null hypothesis that there is no weekly cycle, we need a statistical model for the expected number of storms under the null hypothesis. Since we only test data from portions of a year rather than for full years, we require a model that describes the variation in the expected number of storms as a function of the day of the year. We assume that the expected number of tornado/hail events for a given day and season/year is proportional to the total number of storms for that season (thus capturing the interannual variability in Figure 2) and to the average number of storms for the given day of the year (as represented by the smooth curve in Figure 3). If there is a weekly cycle, we generally assume in our analyses that the cycle is described as a sinusoidal oscillation modulating the expected number given by our null hypothesis model (this is made precise by equations (2) and (3)). Another possible shape for the weekly modulation, a step function, is investigated later.

[26] To represent the expected number of tornados $n_0(y, j)$ in year y and day j for summertime tornados (1 June–31 August, i.e., $152 \leq j \leq 243$) under the null hypothesis, then, we assume that the number is proportional to the number of tornados that summer $n(y)$ and to the seasonal cycle $f(j)$ represented by the smooth curve in Figure 3. Thus,

$$n_0(y,j) = n(y)\frac{f(j)}{\sum_{j'=152}^{243} f(j')}. \tag{1}$$

If $n(y, j)$ is the actual number of observed storm occurrences in year y for day j, $j = 1, \ldots, 365$ (or 366 in a leap year), we define the ratio variable

$$r(y,j) = n(y,j)/n_0(y,j), \tag{2}$$

which has an average very near 1 when averaged over all years of data, or when averaged over all j, by construction. (Hailstorm statistics are similarly treated, using the climatology of hail based on the years 1980–2009.)

3.2. Statistical Model of Weekly Cycle

[27] We determine whether there is a weekly cycle in the ratio variable $r(y, j)$ by fitting the time-dependent data $r(t)$ to a 7 day sinusoid

$$r(t) = r_0 + r_7 \cos[\omega_7(t - \varphi_7)] + \varepsilon(\mathrm{t}), \tag{3}$$

with $\omega_7 = 2\pi/7$ days, where r_0 is the mean of the ratio variable, r_7 is the amplitude of the cycle, and φ_7 is the time during the week when the weekly cycle peaks. The error in the fit is denoted by $\varepsilon(t)$. The time t is measured in days starting from an arbitrary date (we used $t = 0$ on Tuesday, 1 January 1980).

[28] Statistical tests for the fit depend to some extent on an implicit assumption that the statistics of $r(t)$ do not change with the year or month. Although this is difficult to check with a short time series, we have tried to do this using some tests that seem likely to expose such a variation if it exists. We examined the variance of $r(t)$ calculated from the daily values of $r(t)$ over the 92 days of a single season, and plotted the variance versus the number of observed tornados for that season, and did not see signs of a change in the variance from those summers with relatively few tornados compared with those with many. We also examined the variance of $r(y, j)$ for each Julian day j, $j = 1, \ldots, 365$, over the 30 years of data $y = 1980$–2009. When the variance is plotted versus the mean tornado count for a given day j, denoted above by $f(j)$, we find that the variance declines with the tornado count approximately as $f(j)^{-0.62}$. Since $f(j)$ itself only varies by approximately a factor of 3, this suggests that the variance of $r(t)$ ranges only over about a factor of 2 in size. Although we could adjust our statistical analysis to try to accommodate this possible variation, it would be at the cost of considerably more complexity in the analysis and very little gain in knowledge. The bootstrap analysis method described later also tends to circumvent the assumption of homogeneity of the statistics of $r(t)$, though not entirely.

[29] It is perhaps worth reminding the reader here that by fitting the data to a pure sinusoid (equation (3)) we are not assuming that this is in fact an exact description of the weekly cycle in the data. A periodic signal with period 7 days can always be expressed as a sum of sinusoids with periods of 7 days and their higher harmonics. The higher harmonics tend to be noisier and harder to estimate from small amounts of data, and we have chosen not to examine them. Because the sinusoid is fit using data from all days of the week, the sinusoid makes better use of the data (generating more robust statistics) than a search for a weekly cycle that uses only averages of data from single days of the week, a practice that is fairly common in searches for weekly cycles in data. It is easy to obtain averages for each day of the week and to estimate the uncertainty in the averages using standard statistical techniques. (An example is shown in Figure 4, to be discussed later.) However, unless one has an a priori hypothesis about which days of the week are likely to be anomalously high or low, the investigator must first examine the averages for each day of the week, and then decide which averages are representative of the weekly high and low values of a putative weekly cycle, and finally carry out an a posteriori statistical test to see if the difference of the selected pair of averages is "statistically significant." In effect one has examined 21 pairs of averages and chosen the pair most likely to have a statistically significant difference. Carrying out such an a posteriori test is not completely straightforward, since the prior examination of 21 pairs of (probably correlated) averages must be included in the estimation of the statistical significance of the largest difference. This type of approach generally has lower statistical power in detecting a weekly cycle than the test for a sinusoidal variation in the averages, which entails testing only a single parameter, the amplitude r_7 of the cycle, to ascertain whether there is an anomalous cycle. *Hasselmann* [1979] provides a thorough discussion of why multivariable testing for anomalous averages has less statistical power than testing a single weighted average over

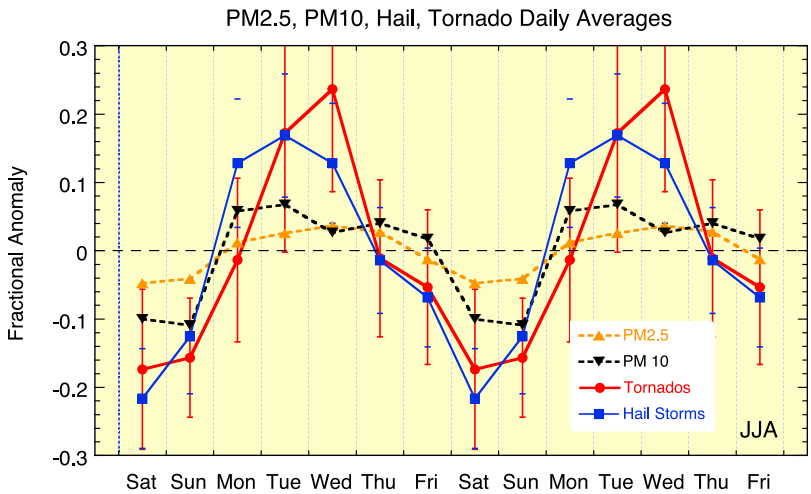

Figure 4. Weekly cycle of the aerosols ($PM_{2.5}$ and PM_{10}), as measured by the Environmental Protection Agency (EPA) over the United States during JJA of 1998–2005 east of 100°W within the continental United States, along with the associated weekly cycle of the Storm Prediction Center–reported hailstorms and tornados over the same area averaged over JJA for 1995–2009. The value shown for each day of the week, for tornado and hail, is a straightforward average of the recorded occurrences for that day of the week, expressed as a fractional anomaly (the deviation of the average from the 7 day mean divided by the mean). The values shown for PM data are averages over all sites of the fractional anomalies computed at each EPA site for which there are data. The significance levels p for the weekly cycle of tornados are $p = 0.011$ (F test) and $p = 0.033$ (bootstrap test). The significance levels for the hail data are $p = 0.00013$ (F test) and $p = 0.0008$ (bootstrap tests with 10^4 simulated data sets). The error bars for the hail are shown only as short horizontal blue lines. The plots repeat the first 7 days in order to better display the nature of the weekly variations.

all variables. See also the discussion of multihypothesis testing by *Wilks* [2006].

[30] A still more powerful test for a weekly cycle might be done if the precise shape of the weekly cycle can be guessed. For instance, one might imagine that the weekly cycle consists in a constant daily average for the weekend (Saturday–Sunday) and another constant average for the weekdays (Monday–Friday, i.e., a step function response), though it is far from obvious that such a response is likely to be an accurate description. We have tried such a test, and the statistical significance of such a postulated cycle is similar in size to the significance we calculate for a sinusoidal weekly cycle (these results are reported later, in section 4.1).

3.3. Statistical Tests for Weekly Cycle

[31] We write $r_7 \cos[\omega_7(t - \varphi_7)] = c_7 \cos(\omega_7 t) + s_7 \sin(\omega_7 t)$ and use linear least squares fits to this expanded version of equation (3) for each of the n weeks of data to obtain the coefficients $c_7(i)$ and $s_7(i)$ for each week i of data, $i = 1, \ldots, n$. Each summer contains 13 weeks of data; for the 15 summers in 1995–2009, there are $n = 15 \times 13 = 195$ weeks of data. The variance of the coefficients $c_7(i)$ and $s_7(i)$ from week to week over the n weeks can be used to estimate the overall uncertainty σ_7 in the amplitude r_7, using σ_7^2 = (variance $[c_7(i)]$ + variance$[s_7(i)]$)/n, where we assume that the correlation of the coefficients from week to week is negligible and the number of samples (n weeks) for variance estimates is large enough that the coefficients c_7 and s_7 are approximately normally distributed. (We tested the time correlations of the fitted amplitudes from week to week and found the correlations to be statistically consistent with the assumed correlation 0.) As explained in more detail by *Bell et al.* [2008], the ratio $(r_7/\sigma_7)^2$ has a Fisher F distribution [e.g., *Fraser*, 1958, p. 202] with two degrees of freedom in the numerator and $(2n - 2)$ degrees of freedom in the denominator. The quantity r_7/σ_7 is a measure of the signal strength (signal-to-noise ratio). The significance level p of the amplitude r_7, under the null hypothesis that there is no weekly cycle, can be fairly accurately estimated from this ratio as

$$p = \exp\left[-(r_7/\sigma_7)^2\right], \tag{4}$$

as explained in much more detail by *Bell et al.* [2008]. The estimate (4) gives nearly the same result as the more complex Fisher F distribution. Note that this means that the probability that r_7 is larger than 1.73 σ_7 is $p = 0.05$; in other words, for tests of the significance of r_7 the threshold for significance is 1.73 σ_7 instead of the familiar 2σ estimate 1.96 σ_7 that the traditional normal distribution would suggest.

[32] Note that the coefficient r_7 in equation (3) is obtained by fitting all of the data, following the same procedure described above that was used for each week of data, and is related to the best fit coefficients c_7 and s_7 by the formula $r_7^2 = c_7^2 + s_7^2$. The phase φ_7 is obtained from $[7/(2\pi)] \tan^{-1}(s_7/c_7)$ measured in days. Since $t = 0$ is a Tuesday in our scheme, the phase φ_7 is measured relative to a Tuesday.

[33] Because of the normalization of the observed number $n(y, j)$ by the expected number $n_0(y, j)$ in equation (2), the value of r_0 in (3) obtained by the fitting procedure is typically very close to 1. (It is not exactly 1 because the seasonal

cycle $f(j)$ is based on an average over all years (1980–2009) whereas our fits generally use only the years 1995–2009.)

[34] The statistical significance of the amplitude r_7 is estimated both by the method described above and by a second method. The second method of estimating the statistical significance of the fitted amplitude r_7 uses a bootstrap approach in which the original data are resampled in segments 11 days long in a way that destroys any 7 day periodicity in the original data. Segment sizes of 11 days are used based on the belief that the correlation of weekly cycle fits to the segments from one segment to the next is small. Where we have checked, it is indeed small. For example, the week-to-week lagged correlations of the coefficients $c_7(i)$ and $s_7(i)$ calculated using the tornado data (east of 100°W) for the 30 summers of 1980–2009 are found to be Corr[c_7, c_7] = 0.046, Corr[s_7, s_7] = −0.114, and Corr[c_7, s_7] = −0.0077; for the hail data they are Corr[c_7, c_7] = 0.032, Corr[s_7, s_7] = −0.014, and Corr[c_7, s_7] = −0.0051. Since there are about 390 weeks of data for this period, the 5% (2σ) significance threshold level for correlations is approximately $2\sqrt{390}$ = 0.10. Only one of the six correlations passes this threshold, barely. The hypothesis that the week-to-week correlations of the fits are zero can therefore not be rejected.

[35] To randomize with respect to the day of the week, segments are selected that are displaced from the original segment anywhere from 7 days before to 6 days after the original segment (i.e., whose starting point is chosen from within a 14 day window). We choose segments from prior or future seasons up to 5 years away, instead of confining ourselves to data from the same year, to increase the number of replacement choices. Thus, for example, if the segment we are replacing starts on 10 August 2001, we may randomly select a segment from the original data set beginning anywhere from 3 to 16 August and from any year from 1996 to 2006. This tends to generate simulated data sets with statistics that change with the day of the year in the same way as the original data set, as far as preserving the seasonality of the statistics and decadal trends, but having no real weekly cycles. Note that because we have access to years prior to 1995, we may select random segments from years as early as 1990 when a segment from year 1995 is being replaced. Note that because the statistics of the ratio variable $r(y, j)$ seem to be fairly constant from year to year (as discussed at the end of section 3.2), we create simulated data sets starting with the original data set for $r(y, j)$ rather than of $n(y, j)$ itself, thereby minimizing the impact of seasonal and interannual variability on the statistics of the simulated data sets.

[36] Synthesized data sets assembled from the 11 day segments are used to estimate values of r_7 for each data set, and the statistical significance of the value of r_7 obtained from the original data set is set at the fraction of synthesized data sets with r_7 larger than that of the original value. We found that the two methods produced comparable significance levels p (the probability that the value of r_7 could equal or exceed its value under the null hypothesis $r_7 = 0$).

4. Analysis Results

4.1. Results for Tornados East of 100°W

[37] In accordance with the hypothesis that the impact of air pollution on invigorating severe storms would be greatest in a moist and warm atmosphere, we follow our previous geographic partitioning [*Bell et al.*, 2008, 2009a], and examine data for the summer months, June–August, and areas east of 100°W for all latitudes within the United States (our earlier studies were constrained by the latitudinal coverage of the satellite data we used). The longitude of 100°W separates the moist air mass to the east, where invigoration can be expected, from the dry air masses to the west, where cloud bases are too high and cold to be substantially invigorated by added aerosols. This is evident in the map of climatological mean dew point temperature for July, shown in Figure 1 (top).

[38] Hail and tornado data are available from 1950, but their quality has evolved over time. The completeness of the coverage has been improving, especially, we assume, for the weaker and thus less noticeable events. On the basis of the evidence in Figure 2, overall observational coverage of tornados seems to have stabilized since the mid 1990s, whereas coverage of hail appears to have grown continuously. We have focused our search on the period 1995–2009. This choice is also motivated by the results of *Bell et al.* [2008], where clear signs were reported of a weekly cycle in satellite estimates of rainfall, in rain gauge data, and in the induced modulation of the regional circulation patterns for the period 1998–2005, and where evidence that the weekly cycle seemed to weaken in earlier decades was found.

[39] A weekly cycle in the aerosol impacts on storms depends on the existence of a weekly cycle in anthropogenic aerosols. Ideally one would examine long-term records of the concentration of cloud condensation nuclei (CCN) near cloud base in order to establish the existence of weekly cycles in the aerosols that directly influence storm evolution. Continuous monitoring of CCN concentrations over the geographical scales of interest is not yet available, unfortunately. As an indicator of anthropogenic emission of aerosols, however, we have examined Environmental Protection Agency (EPA) data sets for surface-level concentrations of particulate matter with particle diameters greater than either 10 μm or 2.5 μm, respectively. These data were recently analyzed by *Bell et al.* [2008]. A weekly cycle in both PM_{10} and $PM_{2.5}$ is clearly to be seen in Figure 4. Figure 4 shows the fractional anomalies (deviations from the mean divided by the site mean) observed at each site, averaged over all EPA sites. The weekly cycles of hail and tornadic storms for the years 1995–2009, also shown in Figures 4 and 5, behave very similarly to the cycle in the aerosols, with a distinct minimum on weekends.

[40] When fits to the weekly cycle shown in Figure 4 using sinusoids are tested for statistical significance, the p values (probability of the truth of the null hypothesis that there is no weekly cycle) are small, especially for hailstorms (of which there are many more events than for tornados). As mentioned above (see section 3.2), one can carry out statistical tests for other functional shapes of the weekly cycle response. When we fit the data to a step function with one constant during the weekend and another during the work week, we found the statistical significance (p values) of such a response shape to be similar to what we found for the sinusoid, even though the sinusoid includes an extra parameter, the phase of the cycle. We found that a step function fits the tornado data with a $p = 0.013$ using a Student's t test and $p = 0.015$ from bootstrap estimation. A step function fits the

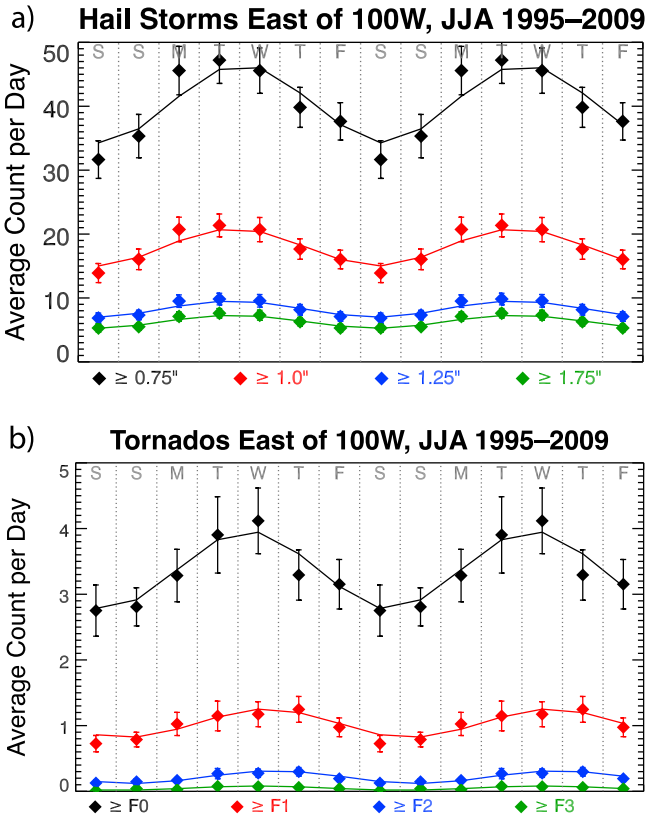

Figure 5. (a) Daily averages for hail occurrences of various strengths (hail diameters) are shown, using data for hailstorms east of 100°W within the continental United States for June–August 1995–2009. Smooth curves are sinusoidal fits to data. (b) Daily averages for tornado occurrences of various strengths (F values) are shown, using data for tornados east of 100°W within the continental United States for June–August 1995–2009. Smooth curves are sinusoidal fits to data.

hail data with a $p = 0.003$ using a Student's t test and $p = 0.0001$ from bootstrap estimation. (When p values get this low, estimates of p values can be very noisy.) Both of these step function fits used data from 1995 to 2009, JJA, for the area east of 100°W. Figure 6 shows plots of the weekly cycles and fits. (The constant portions of the step function fits are not perfectly flat because of the effect of converting $r(t)$ to $n(t)$ using equation (2), since it is $r(t)$ that is fit to the step function but it is averages of $n(t)$ that are plotted in Figure 6.)

[41] The temporal and spatial distribution of the weekly cycle matches the distribution of the warm, moist and unstable conditions in which aerosols have the strongest tendency to invigorate deep convective clouds [*Rosenfeld et al.*, 2008]. During summer, the longitude of 100°W coincides with the transition from the moist climate to the east of it to the hot and dry climate to the west, as shown in Figure 1 (top).

[42] The moisture peaks in the months of June, July, and August and reaches the northeast United States, but starts to retreat southward during late August and September. The aerosol invigoration effect on convective clouds can become apparent in moist atmospheres when synoptic forcing is less dominant. In cool base clouds (i.e., temperature of about 10°C or less) the effect diminishes [*Rosenfeld et al.*, 2008]. This is in agreement with the spatial and temporal distribution of the weekly cycle, as depicted in Figure 7. Figure 7 shows the state of the weekly cycle over three latitudinal bands east of 100°W as a function of the time of year. Each arrow represents the statistics for a 2 month period from the years 1995–2009. The length of the arrow shows the amplitude of the weekly cycle r_7 as a fraction of the mean r_0. The direction indicates the day of the week when the sinusoidal fit peaks. The color indicates the significance level p of the fit, reflecting the signal-to-noise ratio of the fit. Figure 7 shows that the transition from the synoptically forced storms in the spring, when moisture levels are also much lower (Figure 1, bottom), to the more locally unstable storms that form in a moist unstable air mass in the summer is accompanied by an increase in the weekly cycle modulation tending

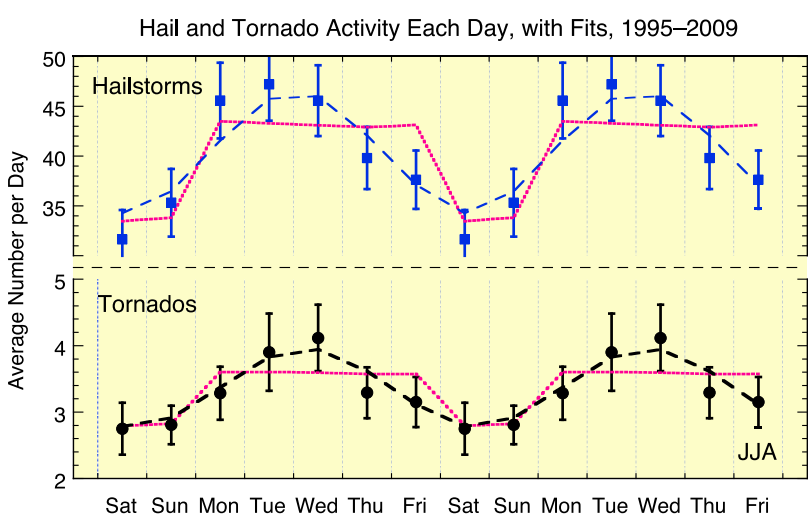

Figure 6. Day-of-the-week averages for tornado and hailstorm occurrences of all strengths, with step function (dotted curve) and sinusoidal (dashed curve) fits superimposed. Error bars are estimated standard errors of averages (i.e., 1σ errors). All events east of 100°W within the continental United States are counted, using June–August 1995–2009 data. Significance levels for fits are given in the text.

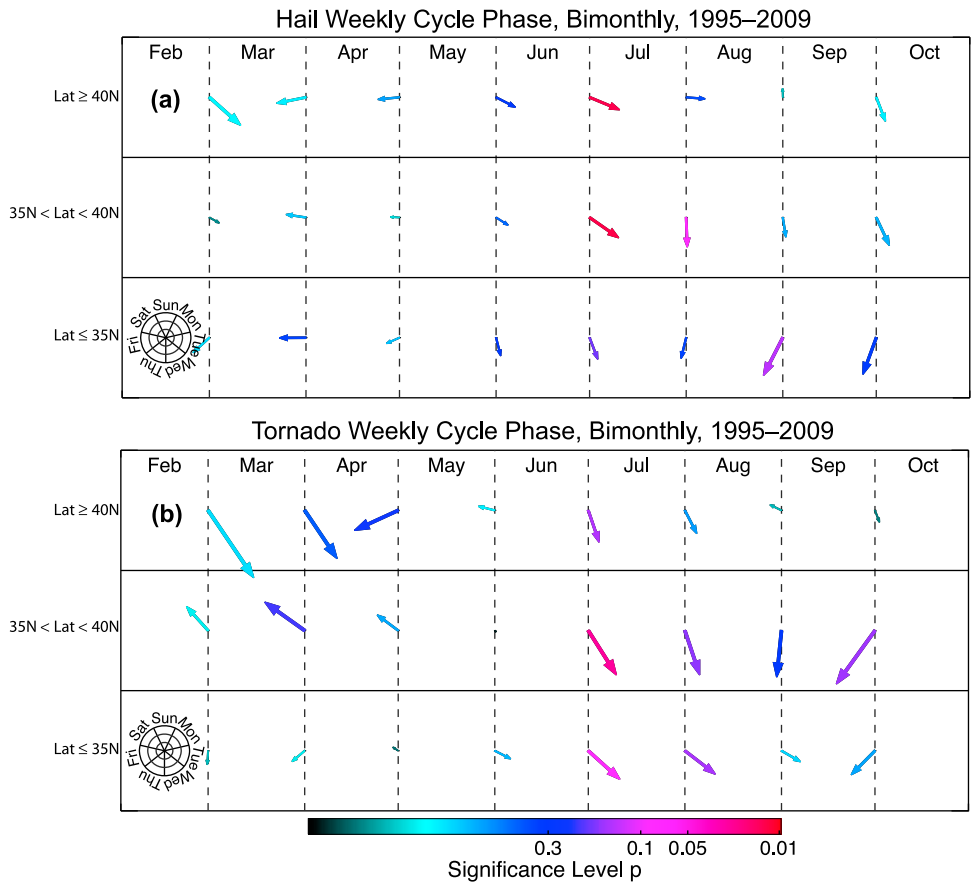

Figure 7. The dependence of the phase of the weekly cycle in (a) hailstorms and (b) tornadic storms on the time of year and geographical latitude (for all storms east of 100°W within the continental United States). Each arrow represents averages of the two months to either side of its location. The latitudes contributing to each row of statistics are shown to the left. The arrow points to the day of the week when the sinusoidal fit is a maximum, and the length indicates the weekly amplitude as a fraction of the bimonthly mean, according to the key at the bottom left. The radius of the outermost circle in the key represents a fractional anomaly of 0.15. The arrows are colored according to their significance level, with the color bar indicating the significance level assigned to each color.

to have a mid-week maximum. The return of the synoptic forcing and drier air in the early fall to the north part of the domain is similarly associated with a decrease of the weekly cycle there. Note that the weekly cycle of tornados only becomes established sometime in June, even though tornadic activity is reaching its peak well before then (see Figure 3). We believe that the consistency of these patterns of occurrence of the weekly cycle in time and space and the predictions of the hypothesis that the pollution aerosols are the cause of the observed weekly cycle in severe convective storms lends additional credence to our hypothesis.

[43] The overall statistical significance of the weekly cycles of tornado and hail activity for the 15 year period 1995–2009 is quite high (see caption to Figure 4). We can also examine the weekly cycle for individual summers based on sinusoidal fits to the data for each summer alone, though the results are noisy given that there are only 13 weeks in a summer. The results of such an analysis were displayed in earlier papers as "clock plots" for rainfall [*Bell et al.*, 2008] and for lightning [*Bell et al.*, 2009a]: the phase and amplitude of sinusoidal fits were used to plot a point on a clock dial running from Saturday to Friday and with the distance of the plot point from the center of the plot proportional to the signal-to-noise ratio of the amplitude. The "noise" σ_7 is determined from the variance of weekly fits to the data. The signal-to-noise ratio r_7/σ_7 is given (see equation (4)) by $[-\log(p)]^{1/2}$, where p is the significance level of the amplitude r_7, i.e., the probability that an amplitude this large could have occurred by chance, due to small-sample effects, when there is in fact no weekly cycle present.

[44] Despite the small number of samples in each summer of data, it was found [*Bell et al.*, 2009a] that the phases of the weekly cycles in lightning activity for summers between 1998 and 2009 fell year after year in the nonweekend sectors of the clock plot. This strongly suggests that the weekly cycle in the data has a period of exactly 7 days and is not an atmospheric wave with a period "in the neighborhood" of 7 days. Because tornado and hail events are not nearly as numerous as lightning events, and the tornado/hail observational coverage not nearly as dense, we would expect the year-by-year clock plots of hail and tornado weekly cycles to be noisier than for lightning. The clock plots for hail and tornados are shown in Figure 8. They cover the years 1995–2009. In order to maximize the weekly cycle signal,

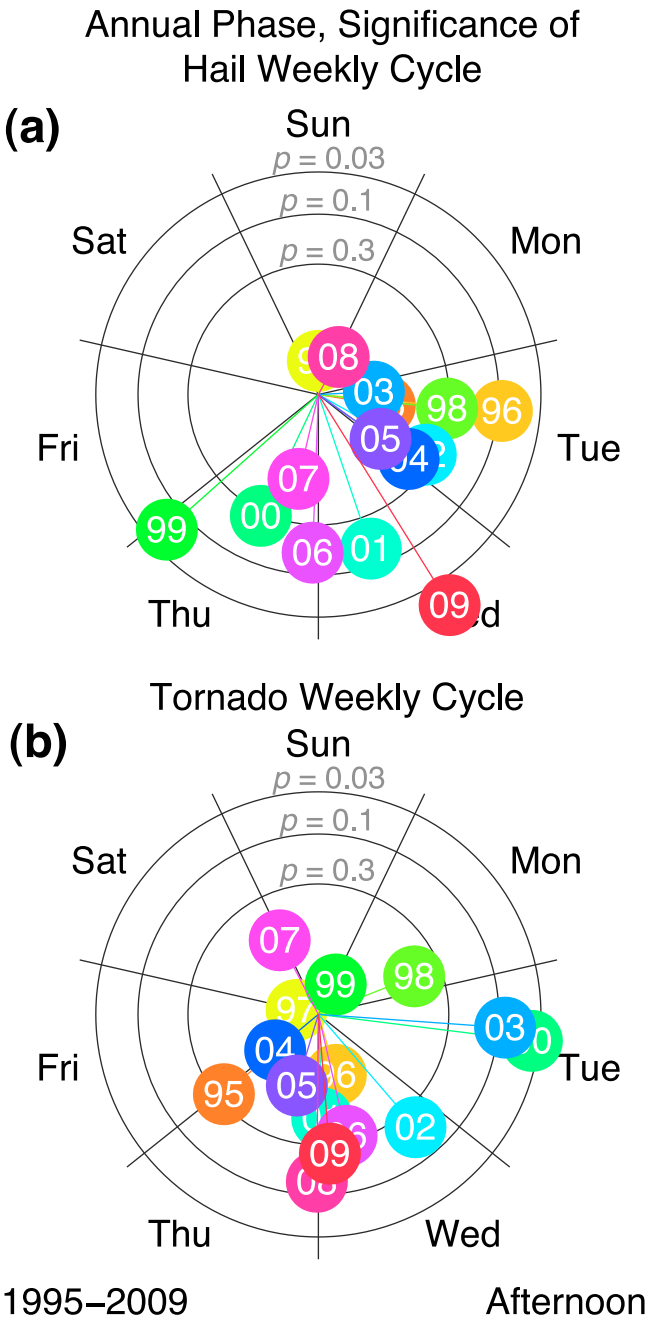

Figure 8. The phase (day of the week) and amplitude of the weekly cycle (equation (3)) of data for each summer for the years 1995–2009. The amplitude is represented by the distance from the origin and is proportional to the signal-to-noise ratio of the amplitude, r_7/σ_7. The last two digits of the year are shown in the colored balloons. The probability p that the amplitude of the weekly cycle could exceed a given radius, under the null hypothesis $r_7 = 0$, is shown by the circles labeled by the corresponding value of p. (a) Hail and (b) tornado data.

only data from the afternoons (1200–2400 local solar time), when convective instability is highest, are used in these plots. Though the phases do not avoid the weekend sectors as completely as the lightning weekly cycle phases did, there is still a clear tendency for the weekly cycles of hailstorms and tornados to peak in the middle of the week. When the phase falls on weekends, the signal-to-noise ratio is quite low, implying that the statistical uncertainty in the determination of the phase is large. Note that the hail data contain about 7 times as many events as the tornado data and therefore have more stable statistics, and the phases are more consistent in avoiding the weekend sectors (Figure 8a).

4.2. Results for Tornados West of 100°W

[45] The average July dew point temperatures are smaller than 10°C at most of the area to the west of 100°W (see Figure 1, top). Therefore we do not expect to find evidence there of weekly storm invigoration. Even though there is a pronounced weekly cycle in aerosols measured by ground-based EPA stations west of 100°W (Figure 9), no significant weekly cycle is apparent to the west of 100°W (Figure 10).

5. Discussion

[46] The results are in agreement with our previous reports of similar weekly cycles in the rainfall [*Bell et al.*, 2008] and lightning [*Bell et al.*, 2009a] over the United States. The cycle was ascribed there to aerosols invigorating deep convective clouds in a warm, moist atmosphere. It is therefore not too surprising to find that the invigorated clouds also produce more hail and tornados.

[47] We show in Figure 8 that the hail and tornado data are consistent with earlier results for rain and lightning in the southeastern United States in another respect: when the phase ϕ_7 and signal strength r_7 for each summer of data for the years 1995–2009 are displayed on a clock plot, there is a clear tendency for the phases to avoid the weekend period, despite the fact that there are only 13 weeks of data in a single summer and estimates of the weekly cycle are quite noisy. It is not surprising that the avoidance is not as clear as it was for the lightning data [*Bell et al.*, 2009a], since lightning occurs far more frequently than hailstorms and tornados and the effective sample size for lightning is far larger.

[48] It is conceivable that the storm data could be affected by a weekly bias in the observations of storms. However, it is shown in Figures 10a and 10b that no sign of a statistically significant weekly cycle in tornado or hail occurrence is visible in the data west of 100°W. If there is a weekly varying bias in storm reports it would have to be present in the eastern half of the United States and absent in the western half to explain our results. Furthermore, the weekly cycle from March to May over the eastern United States (see Figure 7), is not statistically significant, and no longer points to a mid-week maximum. If anything, it is pointing more toward the weekend, but without any statistical significance. This is consistent with the diminution of the convective invigoration effect in cool base clouds, as hypothesized by *Rosenfeld et al.* [2008]. The lack of a clear weekly cycle in the spring along with its existence in the summer, plus the clear correspondence of the weekly cycle that we see in the summer storm data with the cycles observed in other variables with no possible weekly varying observational bias such as lightning, cloud top heights and rain intensities, suggest that the weekly cycle in storms is a real one and not an artifact of the data collection methods.

[49] The weekly cycle that we see is firmly pegged to the work week. It is not plausible that it is a reflection of a

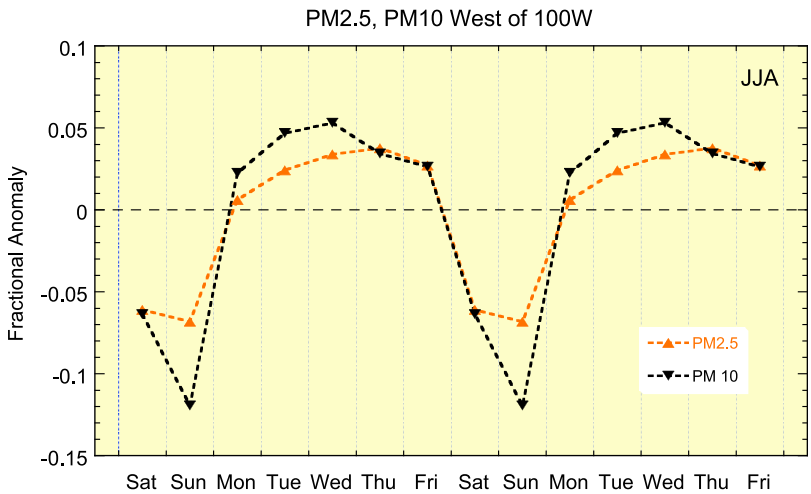

Figure 9. Weekly cycle of the aerosol concentrations ($PM_{2.5}$ and PM_{10}), as measured by the EPA over the United States during JJA of 1998–2005 to the west of 100°W within the continental United States. Daily averages are expressed as fractional anomalies relative to the overall means.

quasiperiodic 7 day cycle in atmospheric dynamics, whose phase would surely wander from year to year, something we do not see in any of the clock plots. *Kim et al.* [2010] recently raised the possibility that the weekly cycle can occur due to natural random variability [*Kim et al.*, 2010]. This might be the case for a weekly cycle that is found in general upper tropospheric synoptic features that have no clear hypothesis to the way that they might be linked to anthropogenic effects [*Sitnov*, 2010]. Weekly cycle in the instability or low-level temperature being larger on weekdays can potentially explain greater the activity of severe convective storms at that time. However, this is not likely to be the case here, based on the lack of evidence of a weekly cycle in the 850 hPa temperatures and in other synoptic properties that correlate with lightning activity that was presented in the supporting online materials of *Bell et al.* [2009a].

[50] An alternative explanation that might be considered is that the radiative effects of the aerosols absorbing and reflecting the solar radiation change the atmospheric stability. If anything, greater aerosol optical depth during mid-week days would reduce the surface heating and suppress convection, as was shown by *Koren et al.* [2004, 2008] and by *Rosenfeld et al.* [2008].

[51] Previous reports of a weekly cycle of hail in Southern France [*Dessens et al.*, 2001] did not show a change in hail frequency, but showed a larger kinetic energy of the hailstones on weekends. It was postulated that ice forming nuclei (IFN) emitted during the week days from the local industry was creating larger number of ice hydrometeors and therefore decreasing the hailstone sizes due to greater competition on the available supercooled water. There is no information whether IFN have a weekly cycle in the eastern United States.

[52] This study has shown a clear correspondence between the weekly cycle of anthropogenic aerosols and the occurrences of severe convective storms, which is highly unlikely to be a result of natural variability. The observed associations cannot serve as proof for causality. However, the results are consistent with the hypothesis that air pollution aerosols invigorate deep convective clouds in moist and unstable

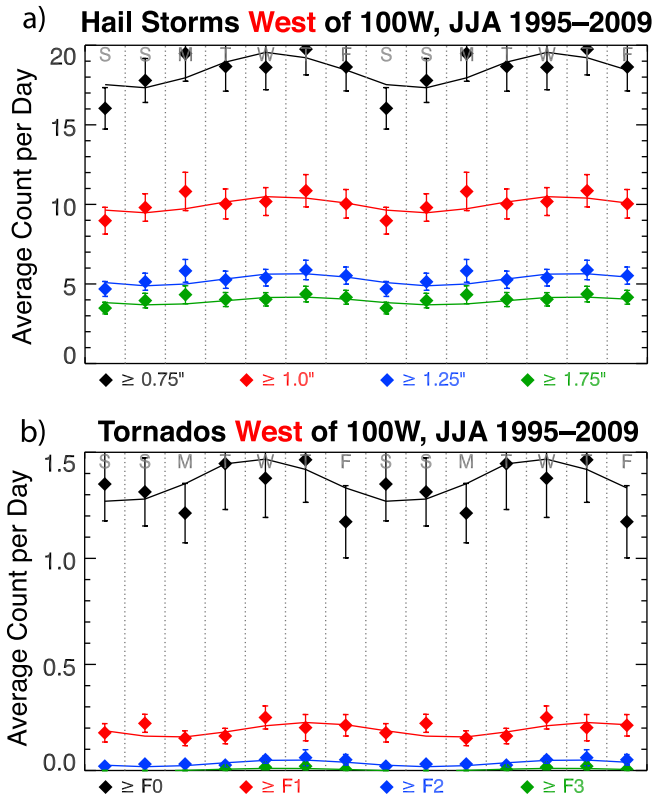

Figure 10. (a) Daily averages for hailstorm occurrences of various strengths (hail diameters) are shown, using data for hailstorms west of 100°W within the continental United States in JJA and for 1995–2009. Smooth curves are sinusoidal fits to data. The weekly cycles are not statistically significant. (b) Daily averages for tornado occurrences of various strengths (EF values) are shown, using data for tornados west of 100°W within the continental United States in JJA and for 1995–2009. Smooth curves are sinusoidal fits to data. The weekly cycles are not statistically significant.

atmosphere, and the possibility that they can even induce the storms to produce large hail and tornados. This is also consistent with the hypothesis that the severe storms are better organized and violent because aerosols increase the hydrometeor size, decreasing their evaporation and so weakening the negative buoyancy of the downdrafts, thereby preventing the gust front from outrunning and undercutting the updraft in the feeder clouds. Anthropogenic emissions have caused large enhancements of aerosol loads even over the remote continents, with typical enhancements of 50–300% over remote regions of Asia, North America, and South America [*Wilson et al.*, 2001; *Chin et al.*, 2004; *Park et al.*, 2006; *Stier et al.*, 2006]. Regarding this increase, it is worth pointing out that if a roughly 10% weekly variation in pollution levels is resulting in a similar change in severe storm activity, then the "background" aerosol level, which is elevated with respect to the preindustrial level even during weekends, is also likely to be changing the storm frequency that we experience today.

[53] **Acknowledgments.** We thank Greg Carbin (NOAA/NWS) for his help in understanding the severe storms data set. We also thank Earle Williams for many helpful comments on the manuscript. Research by D.R. is an outcome of the European Community–New and Emerging Science and Technologies (contract 12444 NEST-ANTISTORM). Research by T.L.B. was supported by the Science Mission Directorate of NASA as part of the Precipitation Measurement Mission program under Ramesh Kakar.

References

Altaratz, O., I. Koren, T. Reisin, A. Kostinski, G. Feingold, Z. Levin, and Y. Yin (2008), Aerosols' influence on the interplay between condensation, evaporation and rain in warm cumulus cloud, *Atmos. Chem. Phys.*, *8*, 15–24, doi:10.5194/acp-8-15-2008.

Andreae, M. O., D. Rosenfeld, P. Artaxo, A. A. Costa, G. P. Frank, K. M. Longo, and M. A. F. Silva-Dias (2004), Smoking rain clouds over the Amazon, *Science*, *303*, 1337–1342, doi:10.1126/science.1092779.

Bell, T. L., D. Rosenfeld, K.-M. Kim, J.-M. Yoo, M.-I. Lee, and M. Hahnenberger (2008), Midweek increase in U.S. summer rain and storm heights suggests air pollution invigorates rainstorms, *J. Geophys. Res.*, *113*, D02209, doi:10.1029/2007JD008623.

Bell, T. L., D. Rosenfeld, and K.-M. Kim (2009a), Weekly cycle of lightning: Evidence of storm invigoration by pollution, *Geophys. Res. Lett.*, *36*, L23805, doi:10.1029/2009GL040915.

Bell, T. L., J.-M. Yoo, and M.-I. Lee (2009b), Note on the weekly cycle of storm heights over the southeast United States, *J. Geophys. Res.*, *114*, D15201, doi:10.1029/2009JD012041.

Brooks, H. E., C. A. Doswell, and M. P. Kay (2003), Climatological estimates of local daily tornado probability for the United States, *Weather Forecast.*, *18*, 626–640, doi:10.1175/1520-0434(2003)018<0626:CEOLDT>2.0.CO;2.

Chin, M., et al. (2004), Aerosol distribution in the Northern Hemisphere during ACE-Asia: Results from global model, satellite observations, and Sun photometer measurements, *J. Geophys. Res.*, *109*, D23S90, doi:10.1029/2004JD004829.

Dessens, J., R. Fraile, V. Pont, and J. L. Sanchez (2001), Day-of-the-week variability of hail in southwestern France, *Atmos. Res.*, *59–60*, 63–76, doi:10.1016/S0169-8095(01)00109-0.

Doswell, C. A., and D. W. Burgess (1988), On some issues of United States tornado climatology, *Mon. Weather Rev.*, *116*, 495–501, doi:10.1175/1520-0493(1988)116<0495:OSIOUS>2.0.CO;2.

Fan, J., R. Zhang, G. Li, and W.-K. Tao (2007), Effects of aerosols and relative humidity on cumulus clouds, *J. Geophys. Res.*, *112*, D14204, doi:10.1029/2006JD008136.

Fan, J., T. Yuan, J. M. Comstock, S. Ghan, A. Khain, L. R. Leung, Z. Li, V. J. Martins, and M. Ovchinnikov (2009), Dominant role by vertical wind shear in regulating aerosol effects on deep convective clouds, *J. Geophys. Res.*, *114*, D22206, doi:10.1029/2009JD012352.

Fraser, D. A. S. (1958), *Statistics: An Introduction*, 398 pp., John Wiley, New York.

Gunn, R., and B. B. Phillips (1957), An experimental investigation on the effect of air pollution on the initiation of rain, *J. Meteorol.*, *14*, 272–280, doi:10.1175/1520-0469(1957)014<0272:AEIOTE>2.0.CO;2.

Hasselmann, K. (1979), On the signal-to-noise problem in atmospheric response studies, in *Meteorology Over the Tropical Oceans*, edited by D. B. Shaw, pp. 251–259, R. Meteorol. Soc., London.

Khain, A., and B. Lynn (2009), Simulation of a supercell storm in clean and dirty atmosphere using weather research and forecast model with spectral bin microphysics, *J. Geophys. Res.*, *114*, D19209, doi:10.1029/2009JD011827.

Khain, A., and A. Pokrovsky (2004), Simulation of effects of atmospheric aerosols on deep turbulent convective clouds using a spectral microphysics mixed-phase cumulus cloud model. Part II: Sensitivity study, *J. Atmos. Sci.*, *61*, 2983–3001, doi:10.1175/JAS-3281.1.

Khain, A., D. Rosenfeld, and A. Pokrovsky (2005), Aerosol impact on the dynamics and microphysics of deep convective clouds, *Q. J. R. Meteorol. Soc.*, *131*, 2639–2663, doi:10.1256/qj.04.62.

Khain, A., N. BenMoshe, and A. Pokrovsky (2008), Factors determining the impact of aerosols on surface precipitation from clouds: Attempt of classification, *J. Atmos. Sci.*, *65*, 1721–1748, doi:10.1175/2007JAS2515.1.

Khain, A., D. Rosenfeld, A. Pokrovsky, U. Blahak, and A. Ryzhkov (2011), The role of CCN in precipitation and hail in a mid-latitude storm as seen in simulations using a spectral (bin) microphysics model in a 2D dynamic frame, *Atmos. Res.*, *99*, 129–146, doi:10.1016/j.atmosres.2010.09.015.

Kim, K.-Y., R. J. Park, K.-R. Kim, and H. Na (2010), Weekend effect: Anthropogenic or natural?, *Geophys. Res. Lett.*, *37*, L09808, doi:10.1029/2010GL043233.

Koren, I., Y. J. Kaufman, L. A. Remer, and J. V. Martins (2004), Measurement of the effect of Amazon smoke on inhibition of cloud formation, *Science*, *303*, 1342–1345, doi:10.1126/science.1089424.

Koren, I., Y. J. Kaufman, D. Rosenfeld, L. A. Remer, and Y. Rudich (2005), Aerosol invigoration and restructuring of Atlantic convective clouds, *Geophys. Res. Lett.*, *32*, L14828, doi:10.1029/2005GL023187.

Koren, I., J. V. Martins, L. A. Remer, and H. Afargan (2008), Smoke invigoration versus inhibition of clouds over the Amazon, *Science*, *321*, 946–949, doi:10.1126/science.1159185.

Koren, I., L. A. Remer, O. Altaratz, J. V. Martins, and A. Davidi (2010), Aerosol-induced changes of convective cloud anvils produce strong climate warming, *Atmos. Chem. Phys.*, *10*, 5001–5010, doi:10.5194/acp-10-5001-2010.

Langenberg, H. (2011), Triggered lightning, *Nat. Geosci.*, *4*, 140.

Lee, J.-S. (1986), Speckle suppression and analysis for synthetic aperture radar images, *Opt. Eng.*, *25*, 636–643.

Lee, S. S., L. J. Donner, V. T. J. Phillips, and Y. Ming (2008a), Examination of aerosol effects on precipitation in deep convective clouds during the 1997 ARM summer experiment, *Q. J. R. Meteorol. Soc.*, *134*, 1201–1220, doi:10.1002/qj.287.

Lee, S. S., L. J. Donner, V. T. J. Phillips, and Y. Ming (2008b), The dependence of aerosol effects on clouds and precipitation on cloud system organization, shear and stability, *J. Geophys. Res.*, *113*, D16202, doi:10.1029/2007JD009224.

Lee, S. S., L. J. Donner, and J. E. Penner (2010), Thunderstorm and stratocumulus: How does their contrasting morphology affect their interactions with aerosols?, *Atmos. Chem. Phys.*, *10*, 6819–6837, doi:10.5194/acp-10-6819-2010.

Lerach, D. G., B. J. Gaudet, and W. R. Cotton (2008), Idealized simulations of aerosol influences on tornadogenesis, *Geophys. Res. Lett.*, *35*, L23806, doi:10.1029/2008GL035617.

Li, G., Y. Wang, and R. Zhang (2008), Implementation of a two-moment bulk microphysics scheme to the WRF model to investigate aerosol-cloud interaction, *J. Geophys. Res.*, *113*, D15211, doi:10.1029/2007JD009361.

Ludlam, F. H. (1963), Severe local storms: A review, in *Severe Local Storms*, *Meteorol. Monogr.*, vol. 27, pp. 1–30, Am. Meteorol. Soc., Boston, Mass.

Lyons, W. A., T. E. Nelson, E. R. Williams, J. A. Cramer, and T. R. Turner (1998), Enhanced positive cloud-to-ground lightning in thunderstorms ingesting smoke from fires, *Science*, *282*, 77–80, doi:10.1126/science.282.5386.77.

Markowski, P. M., J. M. Straka, and E. N. Rasmussen (2002), Direct surface thermodynamic observations within the rear-flank downdrafts of nontornadic and tornadic supercells, *Mon. Weather Rev.*, *130*, 1692–1721, doi:10.1175/1520-0493(2002)130<1692:DSTOWT>2.0.CO;2.

Markowski, P. M., J. M. Straka, and E. N. Rasmussen (2003), Tornadogenesis resulting from the transport of circulation by a downdraft: Idealized numerical simulations, *J. Atmos. Sci.*, *60*, 795–823, doi:10.1175/1520-0469(2003)060<0795:TRFTTO>2.0.CO;2.

Molinié, J., and C. Pontikis (1995), A climatological study of tropical thunderstorm clouds and lightning frequencies on the French Guyana coast, *Geophys. Res. Lett.*, *22*, 1085–1088, doi:10.1029/95GL01036.

Ntelekos, A. A., J. A. Smith, L. Donner, J. D. Fast, W. I. Gustafson Jr., E. G. Chapman, and W. F. Krajewski (2009), The effects of aerosols

on intense convective precipitation in the northeastern United States, *Q. J. R. Meteorol. Soc.*, *135*, 1367–1391, doi:10.1002/qj.476.

Park, R. J., D. J. Jacob, N. Kumar, and R. M. Yantosca (2006), Regional visibility statistics in the United States: Natural and transboundary pollution influences, and implications for the Regional Haze Rule, *Atmos. Environ.*, *40*, 5405–5423, doi:10.1016/j.atmosenv.2006.04.059.

Ray, P. S., P. Bieringer, X. F. Niu, and B. Whissel (2003), An improved estimate of tornado occurrence in the Central Plains of the United States, *Mon. Weather Rev.*, *131*, 1026–1031, doi:10.1175/1520-0493(2003)131<1026:AIEOTO>2.0.CO;2.

Rosenfeld, D., and C. W. Ulbrich (2003), Cloud microphysical properties, processes, and rainfall estimation opportunities, in *Radar and Atmospheric Science: A Collection of Essays in Honor of David Atlas*, *Meteorol. Monogr.*, vol. 52, edited by Roger M. Wakimoto and Ramesh Srivastava, pp. 237–258, Am. Meteorol. Soc., Boston, Mass.

Rosenfeld, D., U. Lohmann, G. B. Raga, C. D. O'Dowd, M. Kulmala, S. Fuzzi, A. Reissell, and M. O. Andreae (2008), Flood or drought: How do aerosols affect precipitation?, *Science*, *321*, 1309–1313, doi:10.1126/science.1160606.

Schaefer, J. T., and R. Edwards (1999), The SPC Tornado/Severe Thunderstorm Database, paper presented at 11th Conference on Applied Climatology, Am. Meteorol. Soc., Dallas, Tex.

Sitnov, S. A. (2010), Weekly cycle of meteorological parameters over Moscow region, *Dokl. Earth Sci.*, *431*, 507–513, doi:10.1134/S1028334X10040203.

Snook, N., and M. Xue (2008), Effects of microphysical drop size distribution on tornadogenesis in supercell thunderstorms, *Geophys. Res. Lett.*, *35*, L24803, doi:10.1029/2008GL035866.

Stier, P., J. Feichter, E. Roeckner, S. Kloster, and M. Esch (2006), The evolution of the global aerosol system in a transient climate simulation from 1860 to 2100, *Atmos. Chem. Phys.*, *6*, 3059–3076, doi:10.5194/acp-6-3059-2006.

Storer, R. L., S. C. van den Heever, and G. L. Stephens (2010), Modeling aerosol impacts on convective storms in different environments, *J. Atmos. Sci.*, *67*, 3904–3915, doi:10.1175/2010JAS3363.1.

Tao, W.-K., X. Li, A. Khain, T. Matsui, S. Lang, and J. Simpson (2007), The role of atmospheric aerosol concentration on deep convective precipitation: Cloud-resolving model simulations, *J. Geophys. Res.*, *112*, D24S18, doi:10.1029/2007JD008728.

van den Heever, S. C., and W. R. Cotton (2004), The impact of hail size on simulated supercell storms, *J. Atmos. Sci.*, *61*, 1596–1609, doi:10.1175/1520-0469(2004)061<1596:TIOHSO>2.0.CO;2.

van den Heever, S. C., and W. R. Cotton (2007), Urban aerosol impacts on downwind convective storms, *J. Appl. Meteorol. Climatol.*, *46*, 828–850, doi:10.1175/JAM2492.1.

van den Heever, S. C., G. G. Carrió, W. R. Cotton, P. J. DeMott, and A. J. Prenni (2006), Impacts of nucleating aerosol on Florida storms. Part I: Mesoscale simulations, *J. Atmos. Sci.*, *63*, 1752–1775, doi:10.1175/JAS3713.1.

Wang, C. (2005), A modeling study of the response of tropical deep convection to the increase of cloud condensation nuclei concentration: 1. Dynamics and microphysics, *J. Geophys. Res.*, *110*, D21211, doi:10.1029/2004JD005720.

Wang, J., S. C. van den Heever, and J. S. Reid (2009), A conceptual model for the link between Central American biomass burning aerosols and severe weather over the south central United States, *Environ. Res. Lett.*, *4*, 015003, doi:10.1088/1748-9326/4/1/015003.

Wilks, D. S. (2006), On "field significance" and the false discovery rate, *J. Appl. Meteorol. Climatol.*, *45*, 1181–1189, doi:10.1175/JAM2404.1.

Williams, E. R. (2005), Lightning and climate: A review, *Atmos. Res.*, *76*, 272–287, doi:10.1016/j.atmosres.2004.11.014.

Williams, E., and S. Stanfill (2002), The physical origin of the land-ocean contrast in lightning activity, *C. R. Phys.*, *3*, 1277–1292, doi:10.1016/S1631-0705(02)01407-X.

Williams, E., et al. (2002), Contrasting convective regimes over the Amazon: Implications for cloud electrification, *J. Geophys. Res.*, *107*(D20), 8082, doi:10.1029/2001JD000380.

Williams, E., V. Mushtak, D. Rosenfeld, S. Goodman, and D. Boccippio (2005), Thermodynamic conditions favorable to superlative thunderstorm updraft, mixed phase microphysics and lightning flash rate, *Atmos. Res.*, *76*, 288–306, doi:10.1016/j.atmosres.2004.11.009.

Wilson, J., C. Cuvelier, and F. Raes (2001), A modeling study of global mixed aerosol fields, *J. Geophys. Res.*, *106*, 34,081–34,108, doi:10.1029/2000JD000198.

Yuan, T., L. A. Remer, K. E. Pickering, and H. Yu (2011), Observational evidence of aerosol enhancement of lightning activity and convective invigoration, *Geophys. Res. Lett.*, *38*, L04701, doi:10.1029/2010GL046052.

Zhang, R., G. Li, J. Fan, D. L. Wu, and M. J. Molina (2007), Intensification of Pacific storm track linked to Asian pollution, 2007, *Proc. Natl. Acad. Sci. U. S. A.*, *104*, 5295–5299, doi:10.1073/pnas.0700618104.

T. L. Bell, Climate and Radiation Branch, NASA Goddard Space Flight Center, Greenbelt, MD 20771, USA.

D. Rosenfeld, Institute of Earth Sciences, The Hebrew University of Jerusalem, Jerusalem 91904, Israel. (daniel.rosenfeld@huji.ac.il)